THREE AXIS CONTROL OF THE HUBBLE SPACE TELESCOPE USING TWO REACTION WHEELS AND MAGNETIC TORQUER BARS FOR SCIENCE OBSERVATIONS

Sun Hur-Diaz,[*] John Wirzburger,[†] and Dan Smith[‡]

The Hubble Space Telescope (HST) is renowned for its superb pointing accuracy of less than 10 milli-arcseconds absolute pointing error. To accomplish this, the HST relies on its complement of four reaction wheel assemblies (RWAs) for attitude control and four magnetic torquer bars (MTBs) for momentum management. As with most satellites with reaction wheel control, the fourth RWA provides for fault tolerance to maintain three-axis pointing capability should a failure occur and a wheel is lost from operations. If an additional failure is encountered, the ability to maintain three-axis pointing is jeopardized. In order to prepare for this potential situation, HST Pointing Control Subsystem (PCS) Team developed a Two Reaction Wheel Science (TRS) control mode. This mode utilizes two RWAs and four magnetic torquer bars to achieve three-axis stabilization and pointing accuracy necessary for a continued science observing program. This paper presents the design of the TRS mode and operational considerations necessary to protect the spacecraft while allowing for a substantial science program.

INTRODUCTION

The Hubble Space Telescope (HST) was launched in April 1990 and since that time has been renowned for its superb pointing accuracy of less than 10 milli-arcseconds absolute pointing error. To accomplish this, the HST relies on its complement of four reaction wheel assemblies (RWAs) for attitude control and four magnetic torquer bars (MTBs) for momentum management. As with most satellites with reaction wheel control, the fourth RWA provides for fault tolerance to maintain three-axis pointing capability should a failure occur and a wheel is lost from operations. If an additional failure is encountered, the ability to maintain three-axis pointing is jeopardized. Over the course of the 18 year operational life of HST, there have been two RWA anomalies on-orbit. Due to the unique ability for HST to support servicing by the Space Shuttle, these two RWAs were replaced in February 1997 and March 2002. With the decommissioning of the Shuttle planned prior to the HST end of life, the ability to service the telescope will be greatly diminished.

In order to prepare for this potential situation, the HST Pointing Control Subsystem (PCS) Team developed a Two Reaction Wheel Science (TRS) control mode. This mode utilizes two

---

[*] Emergent Space Technologies, Inc., Greenbelt, MD 20770. E-mail : sun.hur-diaz@emergentspace.com.
[†] Honeywell Technology Solutions, Inc., Columbia, MD 21044. E-mail: jwirzburger@hst.nasa.gov.
[‡] Lockheed Martin Mission Services, Greenbelt, MD 20770. Email: dsmith@hst.nasa.gov.

RWAs and four magnetic torquer bars to achieve three-axis stabilization and pointing accuracy necessary for a continued science observing program.

With just two operational reaction wheels, there exists one axis where no wheel control is available. Magnetic torquer bars can provide control about the wheel-less axis, but they must also continue to dump momentum from the wheels to prevent wheel speed saturation. Because of the reduced wheel momentum management capability of the bars, the wheel speeds can exceed those from normal operations and must be tolerated by the vehicle and safing systems.

Since the MTBs can only generate a torque in the plane perpendicular to the Earth's magnetic field, no control torque can be generated about the wheel-less axis if the magnetic field aligns with the wheel-less axis. This means that certain maneuvers or attitudes may not be feasible and can lead to an uncontrolled vehicle state. Therefore, careful planning of science attitudes and maneuvers is necessary, and significant modification of the current planning and scheduling tools is foreseen.

Reduced-wheel pointing capability had been considered in other missions as well, notably the Far Ultraviolet Spectroscopic Explorer (FUSE)[1,2,3]. Unlike FUSE, HST can experience significant aerodynamic torque which can be on the same order of magnitude as the gravity gradient torque depending on atmospheric density conditions. HST's pointing requirement is also more stringent which places stricter constraints for the reduced-wheel operations.

This paper presents the design of the TRS mode and the operation considerations necessary to protect the spacecraft while allowing for a substantial science program. This mode can operate with any pair of reaction wheels and assumes four magnetic torquer bars and at least three gyros. The paper begins with a brief background followed by the algorithms and some simulation results. Then key issues in planning and scheduling are discussed.

BACKGROUND

The location and direction of the four RWAs on HST along with the definition of the vehicle frame are shown in Figure 1. The boresight of the telescope is along the +V1 axis.
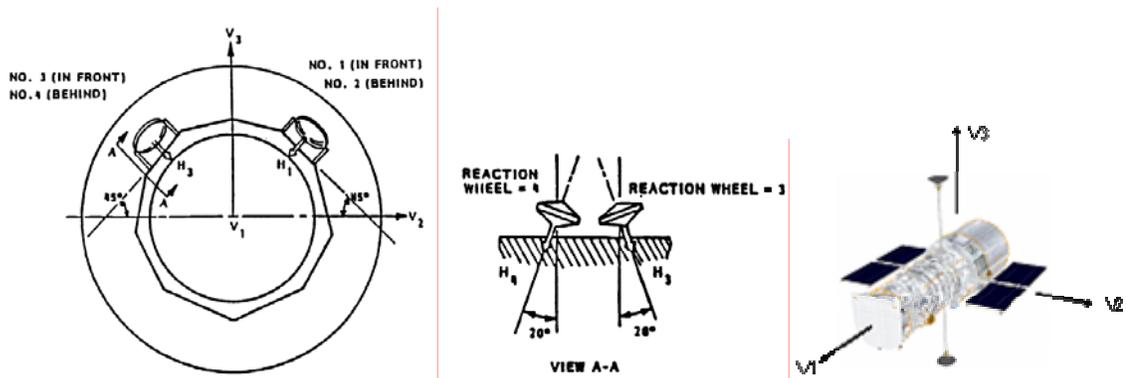

Figure 1 Reaction wheel assembly configuration

There are six possible pairs of wheels that may be in TRS operation. The control authority, hence the performance, depends on the particular pair of reaction wheels used as well as the MTB capability at various levels of aerodynamic torque. The maximum torque from a single wheel is 0.82 N-m for wheel speeds below 3200 RPM. As the wheel speed increases above this value, the torque output begins to diminish. There is also a software limit on the wheel speed for safety.

The torque output from the MTBs depends on their orientation relative to the Earth's magnetic field strength and direction. The maximum dipole moment from a single bar is 3500 amp-meter^2. The maximum torque that can be produced by all four bars is 0.34 N-m. Figure 2 shows the distribution of maximum gravity gradient and aerodynamic torques in the body frame as well as the maximum MTB torque and acceleration capability. The wheel-less axis directions of the six possible pairs of operating wheels are also shown
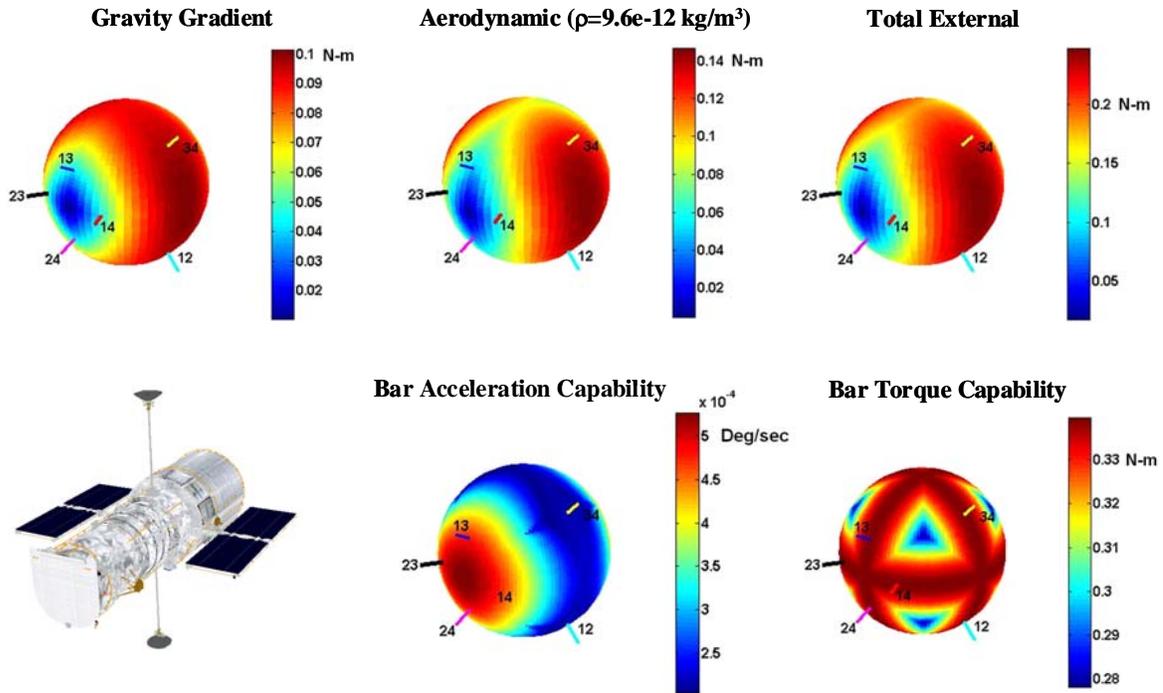

Figure 2 External torque and MTB capability distribution

The MTB acceleration capability distribution shows that wheel pairs (1,2) and (3,4) have the worst control authority about the wheel-less axis as well as the worst external torques. Performance for these two-wheel configurations is expected to be worse than the other four two-wheel configurations.

For adequate control in all three axes, there needs to be enough control authority about the wheel-less axis by the MTBs. This means that certain maneuvers or attitudes may not be feasible and can lead to an uncontrolled vehicle state. Therefore, careful planning of science attitudes and maneuvers is necessary.

In addition to the maximum torque realizable by the MTBs, their dynamics are also important. Figure 3 shows the time response from a PSPICE model of
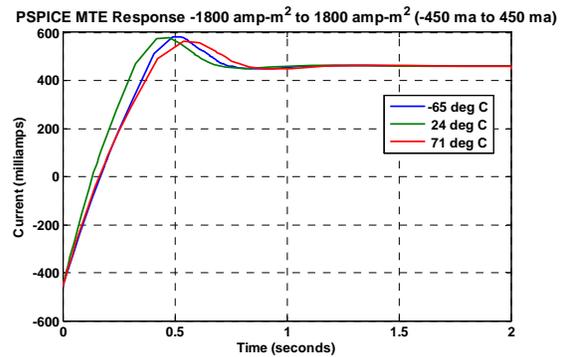

Figure 3 Magnetic Torquer Electronics Time Response

the magnetic torquer electronics at three different temperatures. The general response is that of a second-order system.

To characterize the torque capability about the wheel-less axis, the following parameter is defined:

$$TAWX \equiv \left| \hat{w}_x \cdot \left(-\vec{B}_V \times (T_{Veh/M} \, \vec{\mu}_M) \right) \right| - \left| \hat{w}_x \cdot \left(\vec{T}_{GG} + \vec{T}_{AERO} - \vec{\omega} \times (I\vec{\omega}) - I\vec{a}_{MVR} \right) \right|$$
$$- \left| \hat{w}_x \cdot \left(\vec{\omega} \times (T_{Veh/RWA} \vec{h}_{RWA}) \right) \right| \tag{1}$$

where

$$\hat{w}_x = \text{unit vector in the wheel-less axis in vehicle frame}$$
$$\vec{B}_V = \text{magnetic field vector in vehicle frame}$$
$$T_{Veh/M} = \text{transformation matrix from MTB frame to vehicle frame}$$
$$\vec{\mu}_M = \text{bar dipole moments in MTB frame}$$
$$\vec{T}_{GG} = \text{gravity gradient torque}$$
$$\vec{T}_{AERO} = \text{aerodynamic torque}$$
$$\vec{\omega} = \text{vehicle angular rate in vehicle frame}$$
$$I = \text{vehicle inertia}$$
$$\vec{a}_{MVR} = \text{maneuver acceleration command}$$
$$T_{Veh/RWA} = \text{transformation matrix from wheel to vehicle frame}$$
$$\vec{h}_{RWA} = \text{nominal wheel momentum in wheel frame}$$

A positive TAWX assures controllability about the wheel-less axis. For planning and scheduling purposes, some of the variables are assumed nominal values. For maximum torque from the bars about the wheel-less axis, the bar moments in the above equation are set to

$$\vec{\mu}_M{}^T = \mu_{max} \, sign(\hat{w}_x{}^T [\vec{B}_V]_X \, T_{VM}) \tag{2}$$

where $[\ ]_X$ represents the cross-product matrix of its argument. For maximum wheel gyroscopic torque about the wheel-less axis for a given maneuver axis, wheel momentum is set to

$$\vec{h}_{RWA}{}^T = h_{RWA\_nom} \, sign(\hat{w}_x{}^T [\hat{\omega}]_X \, T_{VW}) \tag{3}$$

During non-maneuver periods, the acceleration command is zero and the two gyroscopic terms containing vehicle angular velocity are negligible. During maneuvers, the acceleration command and the vehicle angular rate are the expected values computed by the maneuver command generator. The expected maneuver attitude profile is also used in the computation of the magnetic field in the vehicle frame as well as the gravity gradient torque and the aerodynamic torque.

ALGORITHMS

One of the main considerations in the design of the TRS mode for HST was to minimize changes to the existing flight software (FSW). Therefore, the existing proportional-integral-derivative control architecture for the normal 3- and 4-wheel modes was left intact as much as possible. A major deviation is the computation of the feedback control in a wheel-orthogonal-frame (WOF) to maximize controllability in the wheel plane. Feedback control is computed in

WOF with gains in the wheel-plane generally higher than the gains in the wheel-less axis since the wheels have higher actuator capability than the bars. Figure 4 illustrates WOF defined by a pair of any two wheels A and B.
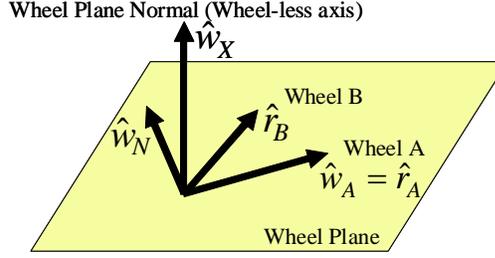

Figure 4 Wheel-Orthogonal-Frame (WOF)

The transformation from the wheel orthogonal frame to the vehicle frame is given by

$$T_{V/WOF} = \begin{bmatrix} \hat{w}_A & \hat{w}_N & \hat{w}_X \end{bmatrix}$$
$$= \begin{bmatrix} \hat{r}_A & \dfrac{\hat{r}_A \times \hat{r}_B}{\left|\hat{r}_A \times \hat{r}_B\right|} \times \hat{r}_A & \dfrac{\hat{r}_A \times \hat{r}_B}{\left|\hat{r}_A \times \hat{r}_B\right|} \end{bmatrix} \tag{4}$$

where the parameters with the "^" symbol indicate unit vectors in the vehicle frame and the other vectors are defined in Figure 4.

TRS Control

Because the MTBs are needed for both vehicle control and wheel momentum management, the primary problem to solve is how to distribute these two potentially competing tasks. Three possible approaches were explored and are described below.

Method 1. The first method takes the feedback control that was transformed to the vehicle frame and sums it with the feedforward control torque compensation comprised of momentum management torque and other known torques. This total torque is used for computing the wheel command as well as for computing the deficit torque, which is the required control torque not achievable by the wheels. The total magnetic dipole command for the torquer bars is computed from a combination of the deficit torque and momentum management torque. The dipole moments of the torquer bars are computed from a modified cross-product law described in a later section.

To include in the feedforward control torque, the momentum management torque is processed through the cross-product law, and the actual momentum management torque that can be produced from the bars is computed as follows:

$$\bar{\mu}_{MM} = \frac{\bar{B}_V \times \bar{T}_{MM}}{\left|\bar{B}_V\right|^2} \tag{5}$$

$$\bar{T}_{MM\_ACTUAL} = \bar{\mu}_{MM} \times \bar{B}_V \tag{6}$$

where $\vec{\mu}_{MM}$ is the dipole moments of the bars also given in the vehicle frame. The negative of this momentum management torque is fed forward along with other known feedforward torques so that the total desired control torque is given by

$$
\begin{aligned}
\vec{T}_C &= \vec{T}_{FB} + \vec{T}_{FF} \\
&= \vec{T}_{FB} - \vec{T}_{MM\_ACTUAL} + \vec{T}_{FF\_OTHERS}
\end{aligned}
\tag{7}
$$

The control torque that is realizable by the wheels is given by

$$
\vec{T}_{CV} = T_{Veh/RWA} \lim_{LIMTRW} \left(T_{RWA/Veh} \vec{T}_C \right)
\tag{8}
$$

where $T_{Veh/RWA}$ is transformation from the wheel frame to the vehicle frame, and $T_{RWA/Veh}$ is the transformation from the vehicle frame to the wheel frame. These transformations are shown below:

$$
T_{Veh/RWA} = \begin{bmatrix} \hat{r}_A & \hat{r}_B \end{bmatrix}
\tag{9}
$$

$$
T_{RWA/Veh} = \left(T_{Veh/RWA}^T T_{Veh/RWA} \right)^{-1} T_{Veh/RWA}^T
\tag{10}
$$

where

$$
\hat{r}_A = \text{unit vector of wheel A in vehicle frame}
$$
$$
\hat{r}_B = \text{unit vector of wheel B in vehicle frame}
$$

Note that the total control torque transformed to the wheel frame is limited by *LIMTRW* before transforming back to the vehicle frame.

The control torque that is not realizable by the wheels is the deficit torque given by

$$
\vec{T}_{DEFICIT} = T_{Veh/WOF} \lim_{TRSLMM} \left[T_{WOF/Veh} \left(\vec{T}_C - \vec{T}_{CV} \right) \right]
\tag{11}
$$

which is to be compensated by the bars as much as possible. The limit *TRSLMM*, applied in WOF, controls how much deficit torque is compensated. The total torque to be produced by the bars is then a combination of the deficit control torque and the momentum management torque. The corresponding bar moment command is then given by:

$$
\begin{aligned}
\vec{\mu}_M &= \lim_{\mu_{MAX}} T_{M/Veh} \left(\vec{\mu}_{DEFICIT} + \vec{\mu}_{MM} \right) \\
&= \lim_{\mu_{MAX}t} T_{M/Veh} \left(\alpha \frac{\vec{B}_V \times \vec{T}_{DEFICIT}}{\left| \vec{B}_V \right|^2} + \vec{\mu}_{MM} \right)
\end{aligned}
\tag{12}
$$

where $T_{M/Veh}$ is the (4x3) transformation from the vehicle frame to the MTB frame, μ_{Max} is the maximum moment limit, and α is a scaling factor applied to achieve the full desired control torque (within the bar limit) and is given by

$$\alpha = \frac{\left|\vec{B}_V\right|^2 \left|\vec{T}_{DEFICIT}\right|^2}{\left|\vec{B}_V \times \vec{T}_{DEFICIT}\right|^2} \tag{13}$$

The scaling of the bar torque is illustrated in Figure 5. With scaling, the projection of the magnetic torque along the deficit torque direction produces the desired magnitude provided that the bars are not saturated. If the magnetic field vector and the deficit torque are aligned, then α is set to 1.
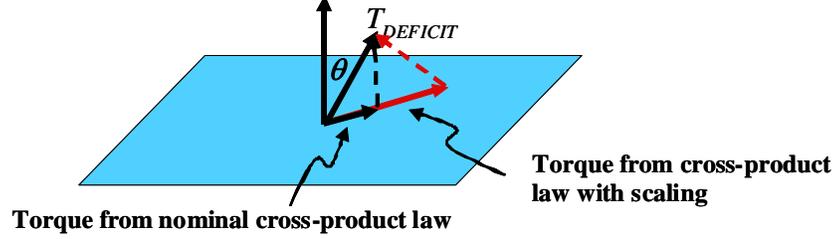

Figure 5 Scaling of the bar torque command for control

Any extraneous torque in the wheel plane produced by the bars is compensated by the wheels. This torque is the desired magnetic torque minus the actual:

$$\vec{T}_{RWA\_MT\_COMP} = -\left(\vec{T}_{DES} - (T_{Veh/M}\,\bar{\mu}_M) \times \vec{B}_V \right) \tag{14}$$

where the desired magnetic torque is given by

$$\vec{T}_{DES} = \vec{T}_{DEFICIT} + \vec{T}_{MM\_ACTUAL} \tag{15}$$

The total command to the wheels is updated with the compensation torque:

$$\vec{T}_{CV} = \vec{T}_{CV} + \vec{T}_{RWA\_MT\_COMP} \tag{16}$$

The total torque to be produced by the wheels is given by the updated command

$$\vec{T}_{RWA} = \lim_{T_{RWA\_Max}} \left(T_{RWA/Veh}\vec{T}_{CV}\right) \tag{17}$$

Method2. In the second method, the desired torque is decomposed into a non-orthogonal UVN frame defined by the unit vector $\hat{n}$ along the intersection of the plane of magnetic control authority and the plane of the wheel control authority which is given by

$$\hat{n} = \frac{\hat{w}_X \times \vec{B}_V}{\left|\hat{w}_X \times \vec{B}_V\right|}, \tag{18}$$

the unit vector in the plane of wheel control authority given by

$$\hat{u} = \frac{\hat{w}_X \times \hat{n}}{\left|\hat{w}_X \times \hat{n}\right|}, \tag{19}$$

and the unit vector in the plane of magnetic control authority given by

$$\hat{v} = \frac{\vec{B}_V \times \hat{n}}{\left| \vec{B}_V \times \hat{n} \right|} \, . \tag{20}$$

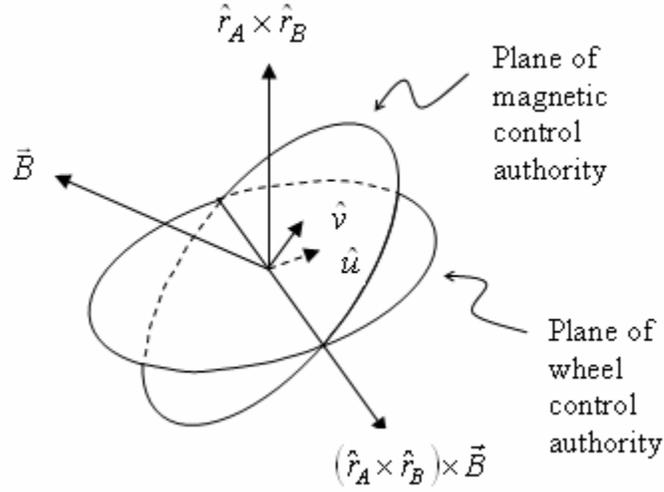Figure 6 illustrates the UVN coordinate frame.

Figure 6 UVN Coordinate Frame

The control torque that is originally computed in the wheel-orthogonal-frame is converted to the vehicle frame and then converted to this non-orthogonal UVN frame as follows:

$$\vec{T}_{uvn} \equiv \begin{bmatrix} T_u \\ T_v \\ T_n \end{bmatrix} = \begin{bmatrix} \dfrac{\vec{T}_V \cdot \hat{u} - (\hat{u} \cdot \hat{v})(\vec{T}_V \cdot \hat{v})}{\left| \hat{u} \times \hat{v} \right|^2} \\ \dfrac{\vec{T}_V \cdot \hat{v} - (\hat{u} \cdot \hat{v})(\vec{T}_V \cdot \hat{u})}{\left| \hat{u} \times \hat{v} \right|^2} \\ \hat{n} \cdot \vec{T}_V \end{bmatrix} \tag{21}$$

The commands to the wheels and the bars are then allocated as follows.

$$\vec{T}_{RWA} = \lim_{T_{RWA\_Max}} T_{RWA/Veh}\left(T_u \hat{u} + T_n \hat{n} \right) \tag{22}$$

$$\vec{\mu}_M = \lim_{\mu_{MAX}} T_{M/Veh}\left(\frac{\vec{B}_V \times T_v \hat{v}}{\left| \vec{B}_V \right|^2} + \vec{\mu}_{MM} \right) \tag{23}$$

The control torque component about the $\hat{n}$ direction (intersection of the wheel plane and the magnetic control authority plane) is allocated fully to the wheels since the wheels have a higher torque capability. The limiting of the bar commands is either proportional for attitude hold or hard for maneuvers.

There is a singularity when the magnetic field vector is aligned with the wheel-less axis. In this case, torque about the wheel-less axis is zero and we only command the control torque in the wheel-plane.

Method3. The third method involves a least-squares solution to optimally combine the wheel torque and the bar torque to produce the desired control torque. Since momentum management torque must be provided by the bars in order to reduce the system momentum, it is not combined with the control torque when using this concurrent method.

The system of equations to solve for is:

$$
\vec{T}_C = \begin{bmatrix} T_{Veh/RWA} & [B_V]_X T_{Veh/M} \end{bmatrix} \begin{bmatrix} \vec{T}_{RWA} \\ \vec{\mu}_{M\_C} \end{bmatrix} \tag{24}
$$

$$
\equiv B\vec{u}
$$

where $\vec{u}$ is the unknown control variable. The above equation represents an under-determined system since there are 6 unknowns and 3 equations, so there is no unique solution. One possible solution is the minimum norm solution which can be solved by forming an objective function augmented with the above equality constraint using a Lagrange multiplier:

$$
\min_{\vec{u}} J = \vec{u}^T W \vec{u} + \vec{\lambda}^T \left(B\vec{u} - \vec{T}_C \right) \tag{25}
$$

where W is a square matrix of weights on the unknowns. We take the partial of J with respect to $\vec{u}$ and $\vec{\lambda}$, set each partial to zero, and solve for $\vec{u}$. After some matrix algebra, we get

$$
\vec{u} = W^{-1} B^T \left(BW^{-1} B^T \right)^{-1} \vec{T}_C \tag{26}
$$

which is essentially a pseudo-inverse of the equality constraint equation. The wheel torque command for control and the bar moment command for control are then given by

$$
\vec{T}_{RWA} = \lim_{T_{RWA\_Max}} \vec{u}(1:2)
$$
$$
\vec{\mu}_{M\_C} = \vec{u}(4:6) \tag{27}
$$

The bar command is limited after the momentum management component is added:

$$
\vec{\mu}_M = \lim_{\mu_{MAX} t} \left(\vec{\mu}_{M\_C} + T_{M/Veh} \vec{\mu}_{MM} \right) \tag{28}
$$

The matrix $BW^{-1}B^T$ is not invertible when the magnetic field is aligned with the wheel-less axis since the rank of the matrix would then be only two. In this case, we can only command the torque in the wheel plane. The pseudo-inverse solution becomes no longer optimal when the control variables begin to saturate and control limits would have to be incorporated. For example, the problem can be posed as a quadratic programming problem with linear and inequality constraints and solved using established nonlinear programming methods.

Comparison of Methods. The three methods of torque allocation presented above were simulated in Matlab. In a case where there is no actuator saturation, all methods performed identically. In a case where there is a period of little or no torque authority about the wheel-less axis, methods 2 and 3 performed worse than method 1. The torque authority for the second case and the attitude errors for all three methods are shown in Figure 7(a) and (b), respectively.
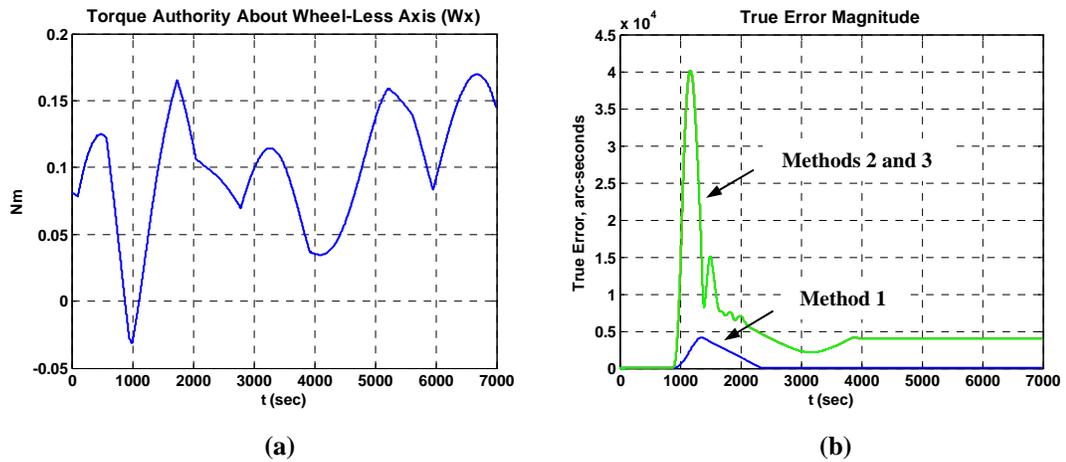
Figure 7 (a) TAWX, (b) Attitude Error

The lighter curve in Figure 7(b) corresponds to methods 2 and 3 whose attitude control error is about 10 times worse than that of method 1. The reason is because the wheels saturate in methods 2 and 3 and thus lose controllability. Figure 8(a) shows the wheel torque history for Method 1, and Figure 8(b) shows the wheel torque history for Methods 2 and 3.
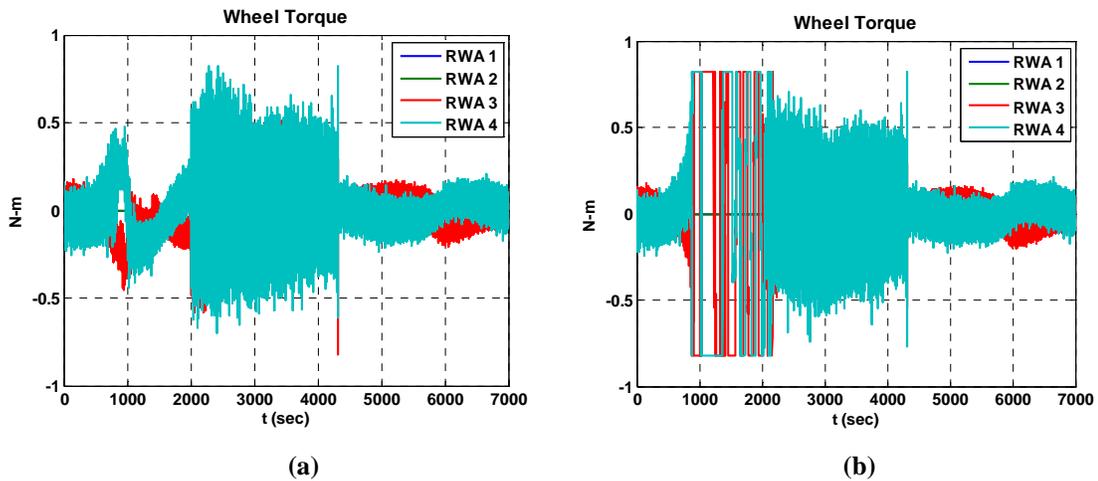

Figure 8 Wheel Torque for (a) Method 1 (b) Methods 2 and 3

For Method 2 or 3 to be viable, actuator limits will have to be addressed. This will be the subject of a future paper.

Momentum Management

For minimal FSW change, the nominal momentum management (MM) proportional-derivative control law is maintained except that the MM command is limited to be only along the direction that would not corrupt control. If the control torque can be fully achieved, i.e., there is sufficient torque authority about the wheel-less axis, then such restriction is not necessary. However, to avoid reducing this torque authority with unnecessary corruption from the momentum management torque, only the $\hat{n}$-component of the nominal momentum management torque, $\vec{T}_{MM}$, is applied:

$$\vec{T}_{MM} = \left(\hat{n}^T \vec{T}_{MM}\right)\hat{n} \tag{29}$$

When the wheel-less axis is aligned with the magnetic field vector within a tolerance, the intersection line is not defined. In this case, most of the realizable momentum management torque is already in the wheel plane and only the component of momentum management torque that is in the wheel plane is commanded.

Maneuver Planning

For maneuver planning in TRS, the same 3- and 4-wheel command generator algorithm is used which is based on an eigen-axis maneuver from an initial attitude to a final attitude. The command generator determines the vehicle rate profile for the control system to follow that satisfies the maximum rate, maximum acceleration, and maximum jerk parameters. For 3- and 4-wheel operations, these parameters are fixed for all maneuvers. For 2-wheel operation, on the other hand, these parameters have to be specified per maneuver because the amount of control authority about the wheel-less axis is dependent on the wheel configuration, the vehicle attitude and orbit, atmospheric density, as well as the magnetic field strength and alignment. The computation of these parameters, which will be performed on the ground by planning and scheduling, is discussed in the next section.

OPERATIONAL CONSIDERATIONS

With just two reaction wheels, there exists one axis where no wheel control is available. Magnetic torque bars can provide control about the wheel-less axis, but they must also continue to dump momentum from the wheels. Because of the reduced wheel momentum management capability of the bars, the wheel speeds can get high. To allow for operation in this mode, the wheel speed safing limit is increased to 4000 RPM from the previous limit of 2800 RPM which still allows for margin for safe mode.

For various operation modes of TRS, the minimum torque authority has to be specified

$$TAWX > TAWX_{Min} \tag{30}$$

Because of the dependency on the aerodynamic drag torque, the minimum torque authority varies with the expected level of the atmospheric density.

Attitude Hold and Science

For attitude hold and science modes, *TAWX* must be sufficient to prevent unallowable attitude errors and maintain RWA momentum adequately to allow for vehicle maneuvers and prevent safemodes. It is obvious that *TAWX* must be greater than 0 N-m at all times during science intervals. Once *TAWX* becomes negative, the external torques become larger than the control torques and the vehicle would incur attitude errors and loss of lock on the target. At 0 N-m, there is no additional torque available for the feedback control loop as all the control torque available is dedicated to controlling expected external torques.

Some attitude error is acceptable during attitude hold portions, as long as the scheduling system protects for the largest error possible. However, once *TAWX* becomes negative, momentum management of the RWAs is no longer guaranteed and wheel speeds increase beyond acceptable limits.

Two major performance criteria are attitude errors and wheel speeds. Figure 9 shows the maximum attitude errors relative to minimum TAWX from a Monte Carlo simulation of 1000 random initial conditions for wheel configuration (1,2) with each case simulated for 3.5 orbits and

with aero density 3.5e-12 kg/m3. Figure 10 shows the wheel speeds relative to the minimum TAWX for all 1000 cases.
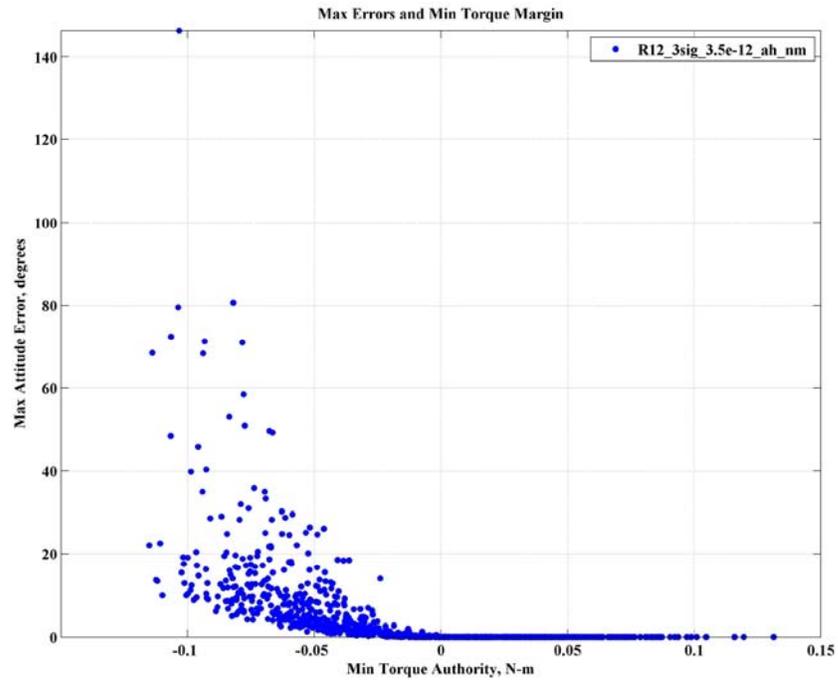
(a)
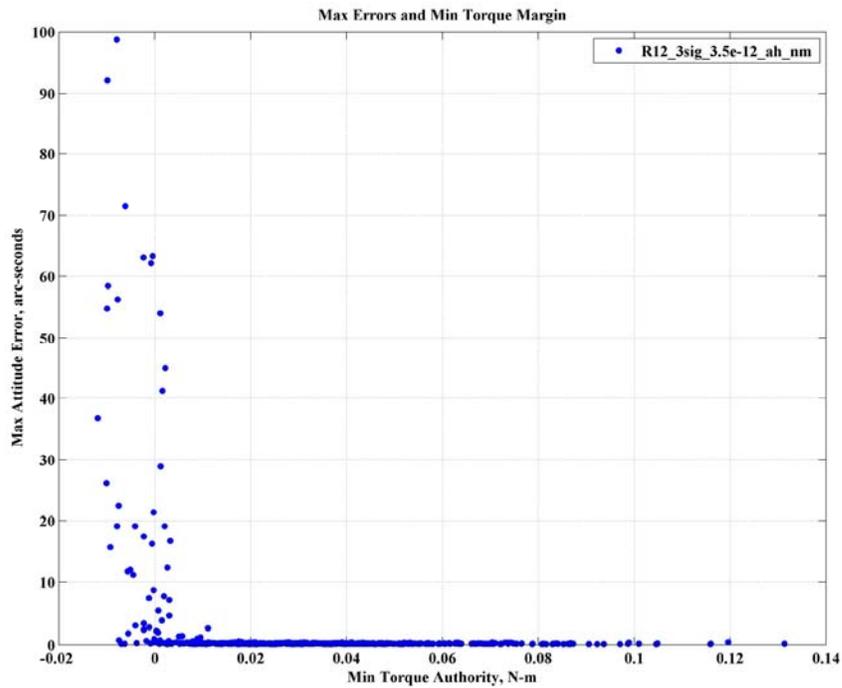
(b)

Figure 9 Maximum attitude error (a) all 1000 cases shown, (b) Close-up
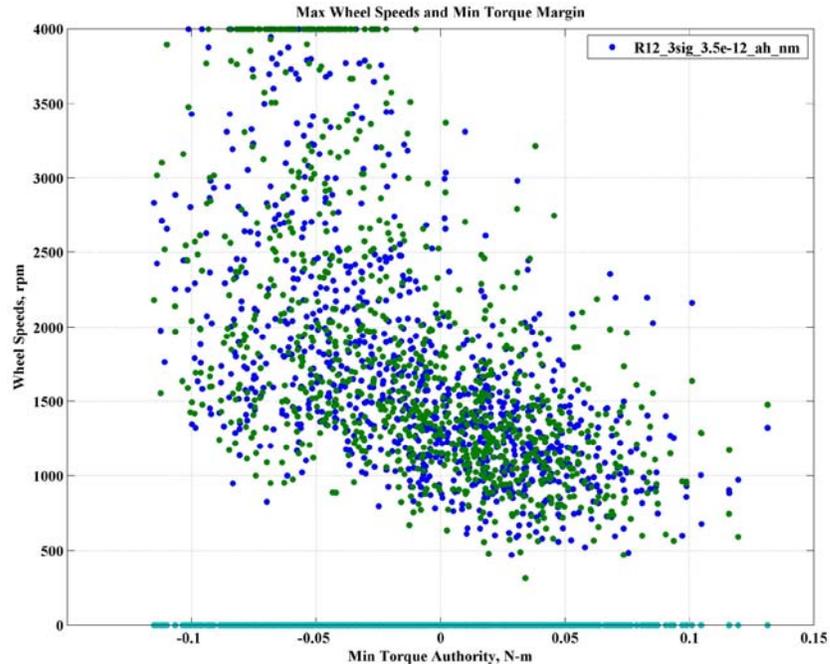
Figure 10 Maximum Wheel Speeds

Based on the simulations, setting $TAWX_{Min}$ to 0.005 N-m would maintain attitude errors below the science acquisition search radii and maintain RWA speeds below the proposed safing speed limit.

Once HST transitions to TRS science mode, the absolute pointing error is maintained below 20 milli-arcseconds for the worst case wheel geometry with the inclusion of attitude information from the Fine Guidance Sensors. This increase in pointing error over the nominal science pointing error with three RWAs of less than 10 milli-arcseconds is primarily due to the lagged response of the MTB as compared to the RWAs.

Figure 11 shows the probability of having a certain torque margin for the entire duration of a 3.5 orbit science observation at a specific time for wheel configuration (1,2) and (1,3) for aero density value of 3.5e-12 kg/m3. As expected, the efficiency is lower for the (1,2) configuration because the torque authority about the wheel-less axis is less. Positive torque margin occurs approximately 40 percent of the time for wheel configuration (1,2) and 60 percent of the time for wheel configuration (1,3).

When performing the calculation of $TAWX$ over attitude hold or science intervals, the selection of atmospheric density is critical. The density chosen must be the maximum density expected to be seen on-orbit during the interval or higher, not a mean value. This ensures torque authority and builds in a slight pad for times when the actual density is lower than the scheduling density. If a mean density value is used, $TAWX_{Min}$ must be reevaluated.
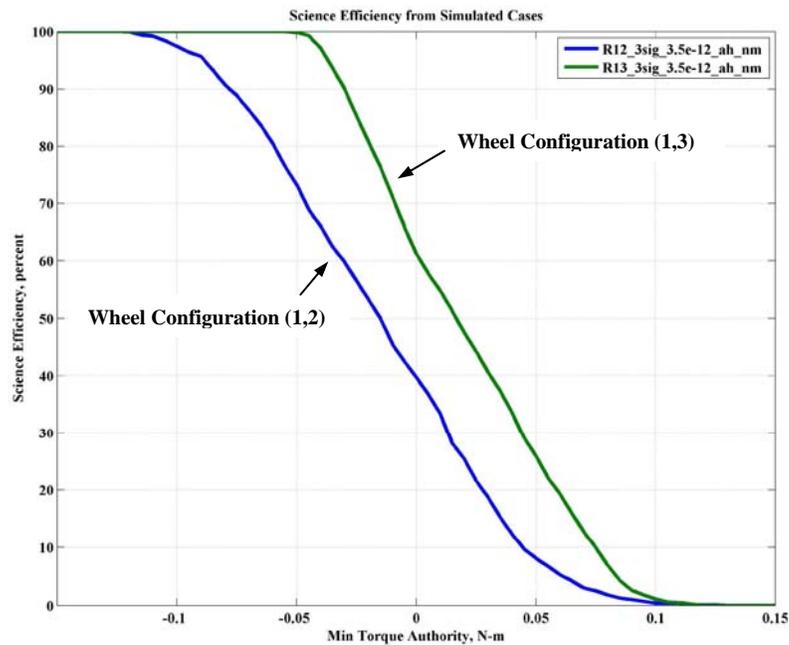
Figure 11 Science Planning Efficiency

One of HST's defining performance characteristics is its jitter level below 7 milli-arcseconds allowing for clear scientific images. Since HST is relatively insensitive to jitter about the boresight axis, this metric is defined as the Root-Summed Squared of the 60-second standard deviation of the pointing error in V2 and V3.

With the increase in actuator rise time incurred by using the MTB as opposed to a RWA, the fine control of HST is degraded. The amount of degradation of jitter is dependent on the remaining two RWAs. The RWA 1-2 and the RWA 3-4 configurations place the wheel-less axis in the V2/V3 plane. This results in the maximum jitter transferred to the boresight as the total affect of the increased jitter due to the MTBs is captured in the jitter calculation. Anticipated jitter levels for the worst-case wheel configurations are on the order of 12 milli-arcseconds, while jitter for the other configurations meets the 7 milli-arcseconds goal. The impact on the science mission due to the increase jitter would be minimal should HST fall into a worst-case wheel configuration.

Similarly, the ability for HST to track a moving target, such as a planet or comet, could be affected. This moving target track makes use of feedforward acceleration to keep the target in the field of view. Through careful gain selection, no significant degradation was observed in moving target tracking.

Through careful design of the attitude hold and science modes, there is minimal performance degradation in TRS mode. However, a transition to TRS is not without cost. The biggest impact to these modes is the ability to schedule attitudes that have sufficient torque margin in the wheel-less axis to control attitude errors and RWA speeds.

Maneuvers

For a given maneuver, the command generator parameters *Vmax*, maximum velocity; *Amax*, maximum acceleration; and *Tstart,* maneuver start time, that satisfy the minimum *TAWX*

requirement will have to be determined. A combination of these command generator parameters that optimizes an objective function, e.g., minimum end-of-maneuver time, can be found:

$$\min_{Vmax,Amax,Tstart} (Tstart + Tslew) \tag{31}$$

subject to

$$TAWX > TAWX_{Min} \tag{32}$$

The parameter *Tstart* is to allow delays in the maneuver for a possible improvement in the magnetic field and orbit, and *Tslew* is the maneuver duration computed in the command generator. The lower and the upper limits of the solve-for command generator parameters in the search space will have to be specified for the various 2-wheel configurations. In addition, the minimum torque-authority about the wheel-less axis $TAWX_{Min}$ has to be specified. Because aerodynamic torque can be a significant torque on the HST, all of these parameters will have to be specified for different levels of atmospheric density.

A method for solving the optimization problem is a global parametric search based on discrete values of the solve-for parameters where each combination of the solve-for parameters is simulated over the maneuver duration. Cases that violate the *TAWX* constraint are rejected, and the combination that minimizes the objective function is selected.

Recall that gyroscopic torque in the computation of *TAWX* in Eqn. (1) is negligible except during maneuvers. Since the momentum of the wheels at the start of a maneuver cannot be predicted, *TAWX* is computed using a nominal wheel momentum value as shown in Eqn. (3). Figure 12 shows plots of *TAWX* from a sample simulation. The top plot shows *TAWX* without the wheel gyroscopic term using nominal values as well as the actual values. The bottom plot shows *TAWX* with the gyroscopic term using a nominal momentum in each wheel of 250 N-m-s as well as the actual wheel momentum. Figure 12 shows the attitude error corresponding to this case.
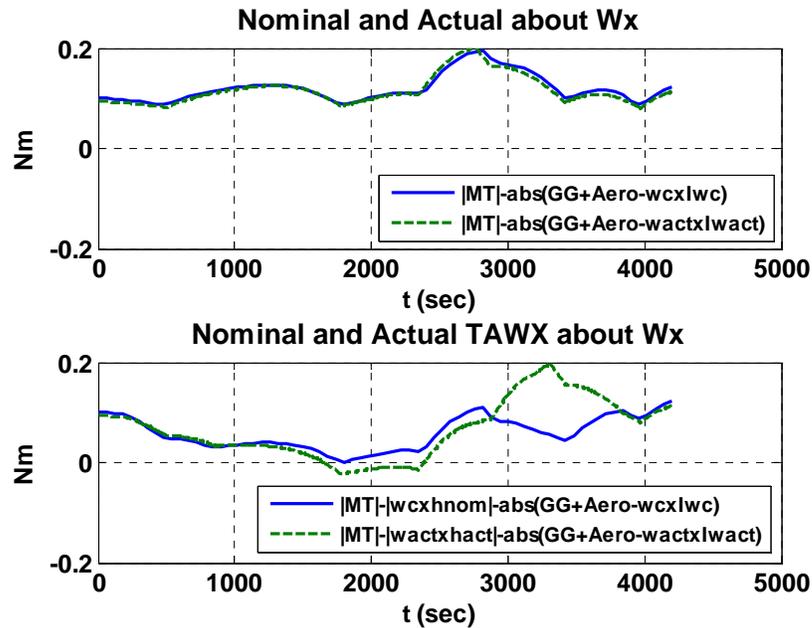

Figure 12 Nominal TAWX using h_{RWA_nom}=250 N-m-s and the actual TAWX for a sample case
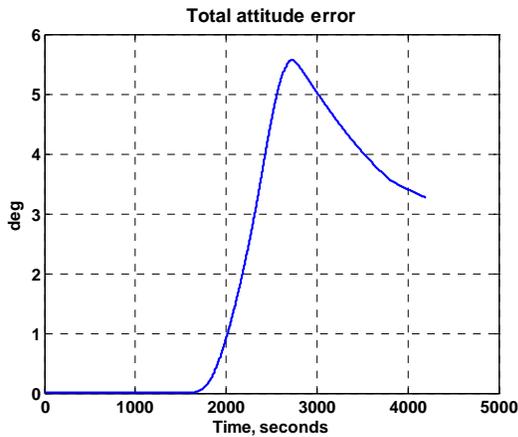
Figure 13 Attitude error corresponding to the case shown in Figure 12

The gyroscopic torque from the unpredictable momentum of the wheels can have a significant effect on the control authority about the wheel-less axis. For this particular case shown, the actual wheel momentum reaches a maximum value of about 350 N-m-s per wheel. To assure that cases such as this are not planned, the optimization problem given by Eqns. (31) and (32) is solved using a larger value of the nominal wheel momentum or a larger value of $TAWX_{Min}$. It is possible that a feasible solution does not exist for a given desired maneuver. If no suitable maneuver exists, the science timeline would have to be modified accordingly.

CONCLUSION

A preliminary design of the two-reaction wheel science (TRS) mode for the Hubble Space Telescope was presented. Three methods of combining wheel torque and magnetic bar torque for TRS control were derived and compared. The first method was chosen for the preliminary TRS design because it has the least impact to the existing flight software code. Without accommodation of actuator limits, the latter two methods perform worse than the first when there is a period of negative torque authority about the wheel-less axis. Consideration of actuator limits in the latter two methods is the subject of a future paper.

Operational considerations in terms of the torque-authority about the wheel-less axis were also presented. Simulation results of both attitude hold and maneuvers show that acceptable performance can be had when there is sufficient torque authority.

ACKNOWLEDGMENT

REFERENCES

1. Roberts, Bryce A., et al, "Three-axis Attitude Control with Two Reaction Wheels and Magnetic Torquer Bars," AIAA Guidance, Navigation, and Control Conference and Exhibit, Paper 5245, Providence, Rhode Island, 16-19 August 2004.

2. Kruk, Jeffrey W., et al, "FUSE In-Orbit Attitude Control with Two Reaction Wheels and No Gyroscopes," SPIE, Vol. 4854, Paper 72, 2002.

3. Sahnow, David J., "Operations with the new FUSE observatory: three-axis control with one reaction wheel," SPIE, Vol. 6266, Paper 2, 2006.